JACC: CARDIOVASCULAR IMAGING VOL. 14, NO. 4, 2021

PUBLISHED BY ELSEVIER

FOCUS ISSUE ON SECONDARY (FUNCTIONAL) MITRAL REGURGITATION

ORIGINAL RESEARCH

Mitral Valve Remodeling and Strain in Secondary Mitral Regurgitation

Comparison With Primary Regurgitation and Normal Valves

K. Carlos El-Tallawi, MD,[a] Peng Zhang, PhD,[b] Robert Azencott, PhD,[b] Jiwen He, PhD,[b] Jiaqiong Xu, PhD,[a,c] Elizabeth L. Herrera, MD,[d] Jessen Jacob, MD,[e] Mohammed Chamsi-Pasha, MD,[a] Gerald M. Lawrie, MD,[f] William A. Zoghbi, MD[a]

ABSTRACT

OBJECTIVES The aim of this study was to assess mitral valve (MV) remodeling and strain in patients with secondary mitral regurgitation (SMR) compared with primary MR (PMR) and normal valves.

BACKGROUND A paucity of data exists on MV strain during the cardiac cycle in humans. Real-time 3-dimensional (3D) echocardiography allows for dynamic MV imaging, enabling computerized modeling of MV function in normal and disease states.

METHODS Three-dimensional transesophageal echocardiography (TEE) was performed in a total of 106 subjects: 36 with SMR, 38 with PMR, and 32 with normal valves; MR severity was at least moderate in both MR groups. Valve geometric parameters were quantitated and patient-specific 3D MV models generated in systole using a dedicated software. Global and regional peak systolic MV strain was computed using a proprietary software.

RESULTS MV annular area was larger in both the SMR and PMR groups (12.7 $\pm$ 0.7 and 13.3 $\pm$ 0.7 cm^2, respectively) compared with normal subjects (9.9 $\pm$ 0.3 cm^2; $p < 0.05$). The leaflets also had significant remodeling, with total MV leaflet area larger in both SMR (16.2 $\pm$ 0.9 cm^2) and PMR (15.6 $\pm$ 0.8 cm^2) versus normal subjects (11.6 $\pm$ 0.4 cm^2). Leaflets in SMR were thicker than those in normal subjects but slightly less than those with PMR posteriorly. Posterior leaflet strain was significantly higher than anterior leaflet strain in all 3 groups. Despite MV remodeling, strain in SMR (8.8 $\pm$ 0.3%) was overall similar to normal subjects (8.5 $\pm$ 0.2%), and both were lower than in PMR (12 $\pm$ 0.4%; $p < 0.0001$). Valve thickness, severity of MR, and primary etiology of MR were correlates of strain, with leaflet thickness being the multivariable parameter significantly associated with MV strain. In patients with less severe MR, anterior leaflet strain in SMR was lower than normal, whereas strain in PMR remained higher than normal.

CONCLUSIONS The MV in secondary MR remodels significantly and similarly to PMR with a resultant larger annular area, leaflet surface area, and leaflet thickness compared with that of normal subjects. Despite these changes, MV strain remains close to or in some instances lower than normal and is significantly lower than that of PMR. Strain determination has the potential to improve characterization of MV mechano-biologic properties in humans and to evaluate its prognostic impact in patients with MR, with or without valve interventions. (J Am Coll Cardiol Img 2021;14:782-93)

From the [a]Houston Methodist DeBakey Heart and Vascular Center, Houston, Texas, USA; [b]Department of Mathematics, University of Houston, Houston, Texas, USA; [c]Center for Outcomes Research, Houston Methodist Research Institute, Houston, Texas, USA; [d]Department of Anesthesiology, Division of Cardiovascular and Thoracic Anesthesiology, Houston Methodist DeBakey Heart and Vascular Center, Houston, Texas, USA; [e]Maimonides Heart and Vascular Institute, Department of Cardiology, Brooklyn, New York, USA; and the [f]Department of Cardiovascular and Thoracic Surgery, Houston Methodist DeBakey Heart and Vascular Center, Houston, Texas, USA. Robert Levine, MD, served as Guest Editor for this paper.

ISSN 1936-878X/$36.00 https://doi.org/10.1016/j.jcmg.2021.02.004

The mitral apparatus is a complex structure consisting of leaflets, a fibrous annulus, papillary muscles, and chordae tendinae. To adequately prevent mitral regurgitation (MR), these structures undergo a synchronized deformation during left ventricular (LV) systole in such a way to optimize anterior (AL) and posterior leaflet (PL) coaptation while minimizing tissue stress. The saddle-shaped dynamic mitral annulus (1–6) plays an essential role toward achieving that goal. In addition, leaflets' size, tissue characteristics, and morphology are other important factors that contribute toward tissue deformation during systolic valve closure. MR is generally divided into a primary etiology (PMR), whereby the valve structure itself is abnormal usually due to myxomatous degeneration, and a secondary etiology (SMR), which is mainly induced by distortion of the mitral apparatus secondary to an abnormal LV geometry. Although most of mitral strain literature is based on animal and in vitro studies (7–12), our recent studies were able to assess mitral valve (MV) deformation dynamics in humans with 3-dimensional (3D) echocardiography acquisitions, using proprietary software developed in our institutions. However, these were pilot studies that tested the feasibility of MV strain in a few patients with PMR and myxomatous degeneration (13,14). Patients with PMR had higher strain compared with normal subjects. There was no assessment of patients with secondary MR.

The advent of current 3D echocardiography with higher spatial and temporal dynamic volumetric imaging, coupled with quick and efficient commercially available tissue tracking software, has allowed for the opportunity to expand this concept to a larger and more diverse patient population. The objective of this study was to quantitate and characterize MV remodeling and patient-specific dynamic MV leaflets deformation noninvasively in patients with SMR in comparison to those with PMR and those with normal MV apparatus serving as control subjects. Global and regional MV strain were compared among these groups, and the correlates of MV strain were evaluated.

ABBREVIATIONS AND ACRONYMS

3D = 3-dimensional
AL = anterior leaflet
LV = left ventricle
LVEF = left ventricular ejection fraction
PL = posterior leaflet
PMR = primary mitral regurgitation
MR = mitral regurgitation
SMR = secondary mitral regurgitation
TEE = transesophageal echocardiography

METHODS

PATIENT POPULATION. The patient population was prospectively enrolled between May 2017 and May 2018 and included subjects who underwent transesophageal echocardiography (TEE) at Houston Methodist Hospital for evaluation of significant native MR. PMR was defined as MR due to leaflet prolapse and/or flail. SMR was defined as MR due to annular dilation and/or leaflet tethering with normal leaflet structure and no evidence of prolapse. Normal subjects were patients who had other nonvalvular indications for TEE (e.g., stroke evaluation in sinus rhythm) where the MV and cardiac structure and function were likely be normal based on a recent transthoracic study. The MV was defined as normal when the MV leaflets had no obvious degenerative changes, namely, there was no evidence of thickening, calcification, mitral annulus calcifications, MR, or other valvular lesions, in the setting of normal LV and left atrial size, LV ejection fraction (LVEF), and LV wall motion in sinus rhythm. Patients with prosthetic valves, MV endocarditis, or suboptimal and/or absent images were excluded from the study (8 studies in total were excluded; n = 2 for normal subjects; n = 6 for PMR). Blood pressure and heart rate were recorded at the time of 3D TEE acquisition. LVEF was determined either from the TEE or from the most recent transthoracic echocardiogram or cardiac magnetic resonance study (most within 7 days of TEE). Baseline demographic and clinical data were obtained at the time of enrollment. The study was approved by the human research review board of Houston Methodist Hospital. All patients provided written informed consent before undergoing TEE.

3-DIMENSIONAL ECHOCARDIOGRAPHY PROTOCOL. Three-dimensional TEE studies were performed on either the EPIQ or iE33 ultrasound systems (Philips, Andover, Massachusetts) using the X7-2t probe. The imaging protocol consisted of a mid-esophageal zoom 3D volume acquisition that included the full extent of the mitral annulus, the anterior and posterior leaflets, and the aortic annulus throughout the cardiac cycle. The acquisition protocol was adjusted for each study to maximize frame rate while maintaining an adequate spatial resolution. This was performed preferentially using multibeat stitched acquisitions or using the high volume rate feature of iE33 and EPIQ machines when the multibeat attempt caused a

The authors attest they are in compliance with human studies committees and animal welfare regulations of the authors' institutions and Food and Drug Administration guidelines, including patient consent where appropriate. For more information, visit the Author Center.

Manuscript received November 24, 2020; revised manuscript received February 8, 2021, accepted February 9, 2021.

FIGURE 1 Stepwise Approach to MV Modeling and Strain Measurement Using 3D TEE

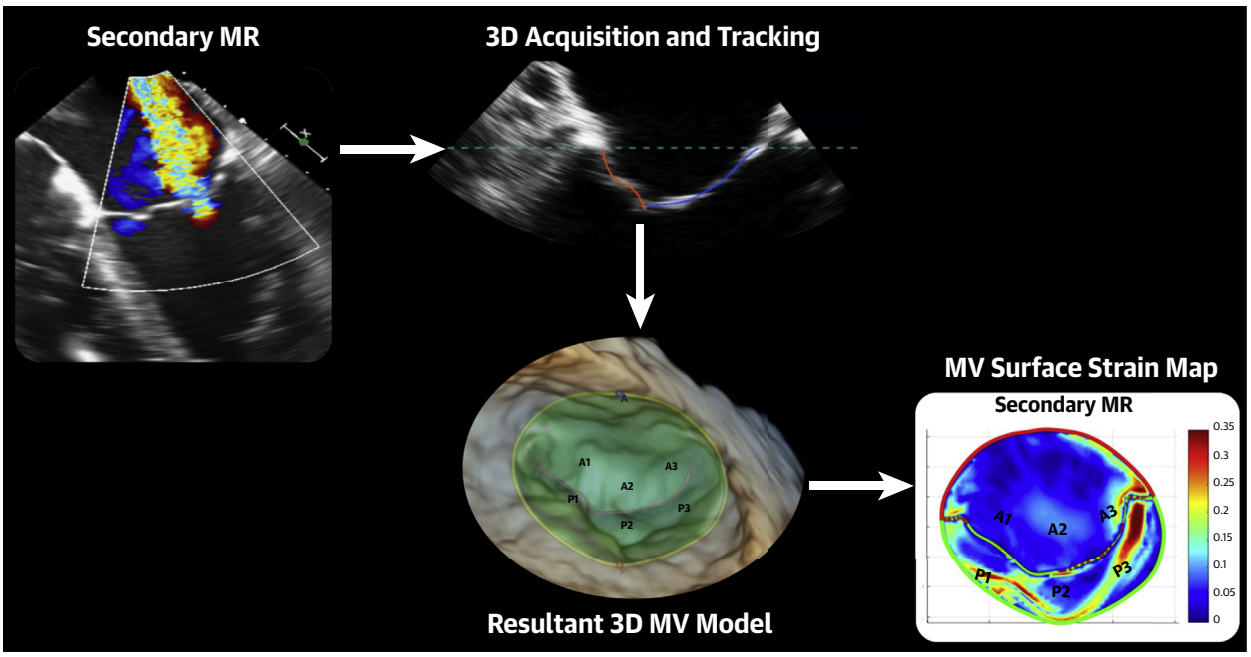

(Top left) Demonstration of the strain calculation process in a patient with secondary mitral regurgitation (MR). **(Top center)** The process begins with 3-dimensional (3D) acquisition and leaflets tracking, followed by **(bottom center)** the creation of a representative mitral valve (MV) model overlaying the 3D acquisition. The numerous mesh points in the model are tracked throughout systole to generate a surface strain heat map from mid- to end-systole **(bottom right)**.
TEE = transesophageal echocardiography.

significant stitching artifact (mean 3D frame rate was 33.5 frames/s). The 3D images were digitally stored as part of each study for post-processing and off-line analysis. MR severity was determined quantitatively from the TEE or a recent transthoracic echocardiogram following calculation of the mitral regurgitant volume, regurgitant fraction, and the effective regurgitant orifice area, or semi-quantitatively using an integrative approach in accordance with the American Society of Echocardiography native valve regurgitation guidelines (15).

PATIENT-SPECIFIC MV TRACKING AND MODELING. Patient-specific models of the motion of the MV annulus and leaflets throughout systole were generated off-line from the 3D TEE datasets using the 4D-MV Assessment software, TomTec Image-Arena version 4.6 (TomTec Imaging Systems, Unterschleissheim, Germany) as depicted in Figure 1. The TomTec software automatically segments out the leaflets and annulus on each 3D image frame throughout systole, with minor operator adjustments afterwards. The resultant MV discretized graphic representations generates a mathematical mesh of 800 to 1,000 points of the MV on each image frame. In addition, each MV model contains the respective total and specific leaflet area, annulus circumference and area, along with annular antero-posterior diameter and height. These basic MV dimensions were acquired at the mid-systolic frame.

LEAFLETS THICKNESS. Anterior and posterior leaflets mean thickness was manually calculated on 4D-MV Assessment software, TomTec Image-Arena version 4.6 software (TomTec Imaging Systems). The 2D contour of each leaflet was traced and its cross-sectional area determined. In addition, the distance between the leaflet tip and its annular insertion (leaflet length) was measured. Mean leaflet thickness was then calculated for each valve as the ratio of leaflet cross-sectional area to leaflet length. These measurements were performed on the 4-chamber (mid-esophageal: zero degrees) and 3-chamber (mid-esophageal: 120 degrees) views; the maximum thickness determination for each leaflet was chosen.

STRAIN COMPUTATION. Diffeomorphic registration has been applied to quantitate ventricular geometry, motion, and myocardial strain (16–19) and has been validated using simulated 3D ultrasound imaging (20) and synthetic ultrasound image sequences (21).

TABLE 1 Baseline Characteristics and Differences Among the Groups

	Normals (n = 32)	Primary MR (n = 38)	Secondary MR (n = 36)	p Value
Age, yrs	55 ± 2.6	69 ± 1.7*	68 ± 2.2†	<0.001
Male	17 (53)	23 (60)	21 (58)	0.71
Hypertension	20 (63)	20 (53)	27 (75)	0.136
CAD	3 (9)	9 (24)	15 (42)†‡	0.01
Diabetes mellitus	6 (19)	7 (18)	10 (28)	0.55
Dyslipidemia	17 (53)	21 (55)	22 (61)	0.79
CKD	5 (16)	6 (16)	17 (47)†‡	0.002
BSA, m^2	2 ± 0.05	2 ± 0.04	2 ± 0.04	0.46
SBP, mm Hg	133 ± 4.1	124 ± 5.0	123 ± 4.4	0.33
DBP, mm Hg	73 ± 2.0§	63 ± 2.1	68 ± 2.5	0.006
HR, beats/min	69 ± 2.4	66 ± 2.0	81 ± 2.7†‡	<0.001
LVEF, %	64 ± 0.6§‖	58 ± 1.6¶	45 ± 2.1	<0.001
Severe MR	0 (0)	26 (68)¶	14 (39)	0.01
Regurgitant volume, ml	N/A	57.1 ± 3.1¶	42.6 ± 2.2	0.003
Regurgitant fraction, %	N/A	47 ± 2	47 ± 2	0.91
Effective regurgitant orifice area, cm^2	N/A	0.42 ± 0.04¶	0.29 ± 0.02	0.045

Values are mean ± SE or n (%). *Primary > normal subjects; $p < 0.05$. †Secondary > normal subjects; $p < 0.05$. ‡Secondary > primary; $p < 0.05$. §Normal subjects > primary; $p < 0.05$. ‖Normal subjects > secondary; $p < 0.05$. ¶Primary > secondary; $p < 0.05$.

BSA = body surface area; CAD = coronary artery disease; CKD = chronic kidney disease; DBP = diastolic blood pressure; HR = heart rate; LVEF = left ventricular ejection fraction: MR = mitral regurgitation; N/A = not applicable; SBP = systolic blood pressure.

Because the 4D-MV Assessment module embedded into TomTec v4.6 does not provide detailed pointwise tracking of mitral leaflet motion, we developed a proprietary software to compute pointwise tracking of leaflets dynamic deformation using diffeomorphic registration between mid- and end-systole (22-24); see the Supplemental Appendix for further details. The software can then compute the mid- to end-systolic tissue isotropic strain IS(x) at roughly 800 MV leaflets points x, with no assumptions on tissue elasticity. For each leaflet point x, and any small leaflet patch P(x) around x, the computed deformation of P(x) between mid- and end-systole roughly multiplies lengths by a dimensionless factor s(x), called the geometric strain at x (24). The isotropic strain IS(x) at x is defined as the magnitude of length dilation (or contraction) around x, given by $IS(x) = |s(x) - 1|$. Therefore, isotropic strain is used to denote the relative multidirectional linear changes of a patch of tissue surrounding point (x), which essentially reflects area deformation between mid- and end-systole. The strain computed at nearly 800 points per leaflet characterize the distribution of IS values on the leaflet surface. These patient-specific strain maps are then graphically displayed on the mid-systolic 3D image of the MV. Strain was quantitated for the AL, the PL, and for the total MV leaflet. Lastly, in the few patients who were in atrial fibrillation at the time of image acquisition, the beat that best represented the average heart rate was picked to calculate strain to minimize the effect of beat-to-beat variability.

PMR COHORT: REGIONAL HIGH-STRAIN CONCENTRATION. To assess the patient-specific highest strain and its localization in both leaflets and regions of the leaflets with or without prolapse and/or flail in the PMR cohort, we defined 6 geometric regions of interest, corresponding to the 3 scallops of the AL and PL (medial, central, and lateral thirds of each leaflet area). This methodology was previously used and explained in detail in our previous publication (13). High strain was defined as strain that was greater than that of the patient-specific 75th percentile. The mean high-strain concentration was computed for each scallop region.

REPRODUCIBILITY. Interobserver and intraobserver reproducibility of MV modeling and strain calculations were performed in a total of 10 cases (random selection in each group: 3 normal subjects, 4 with PMR, and 3 with SMR). Interobserver and intraobserver strain values for the ALs and PLs, as well as total MV strain were compared and correlated.

STATISTICAL ANALYSIS. For each patient and each MV leaflet, we systematically computed 50 quantiles of the patients' leaflet strain values. This enabled the comparison of strain distributions between patients, both within and across patient groups. To quantify similarity or dissimilarity between any 2 strain distributions, we implemented the classic Kolmogorov-Smirnov test. Strain percentiles were computed from strain values at 800 points per patient leaflet. These values were weakly correlated, so our Kolmogorov-

TABLE 2 MV Geometric Variables and Differences Among the Groups

	Normals	Primary MR	Secondary MR	p Value
MV annulus				
Area in projection, cm^2	9.93 ± 0.32	13.32 ± 0.74*	12.73 ± 0.72†	0.001
Circumference, cm	11.68 ± 0.19	13.43 ± 0.36*	13.01 ± 0.37†	0.001
Height, cm	0.77 ± 0.03	0.83 ± 0.05	0.73 ± 0.04	0.21
A-P diameter, cm	3.34 ± 0.07	3.79 ± 0.10*	3.79 ± 0.12†	0.003
Annular area change, %	14.8 ± 0.96‡§	8.2 ± 0.69	6.6 ± 0.66	<0.001
MV leaflets				
AL thickness, mm	1.63 ± 0.05	2.57 ± 0.11*	2.55 ± 0.09†	<0.001
PL thickness, mm	1.99 ± 0.08	3.1 ± 0.12*‖	2.78 ± 0.09†	<0.001
AL area, cm^2	6.44 ± 0.21	7.23 ± 0.41	8.49 ± 0.45†¶	0.002
PL area, cm^2	5.17 ± 0.22	8.35 ± 0.55*	7.71 ± 0.49†	<0.001
Total leaflets area, cm^2	11.6 ± 0.4	15.6 ± 0.8*	16.2 ± 0.9†	<0.001
Leaflets area ratio (PL/AL)	0.82 ± 0.04	1.21 ± 0.07*‖	0.92 ± 0.04	<0.001

Values are mean ± SE. *Primary > normal subjects; $p < 0.05$. †Secondary > normal subjects; $p < 0.05$. ‡Normal subjects > primary; $p < 0.05$. §Normal subjects > secondary; $p < 0.05$. ‖Primary > secondary; $p < 0.05$. ¶Secondary > primary; $p < 0.05$.

AL = anterior leaflet; A-P = anterior-posterior; MV = mitral valve; PL = posterior leaflet; other abbreviation as in Table 1.

Smirnov tests took into account correlations to compare strain percentiles across patients (25). Values of demographic data and geometric parameters are expressed as mean ± SE. Overall difference between the total groups was tested using the 1-way analysis of variance test for continuous variables and the chi-square test for categorical variables. Differences in means for demographic data, MV geometric, and MR severity data, in addition to total and per leaflet mean strain data, among the 3 groups were tested using the 1-way analysis of variance. When there was an overall significant difference, the Bonferroni multiple comparison test was used to account for the multiple comparisons. Univariable and multivariable linear regression analysis were performed to assess determinants of MV strain with clinical and MV geometric parameters. All statistics were performed using Stata Statistical Software Release 16 (StataCorp, College Station, Texas). Statistical significance was defined as 2-tailed $p < 0.05$ for all tests.

RESULTS

PATIENT POPULATION. The study population included a total of 106 subjects: 36 patients with SMR, 38 patients with PMR, and 32 subjects with normal MVs. Table 1 details the demographics and general echocardiographic findings of the 3 groups. Of the 36 patients with SMR, 14 had severe and 22 had moderate MR. Most had nonischemic etiology (n = 25), and 11 had ischemic MR with leaflet tethering associated with regional wall motion abnormalities. Of the 38 patients with at least or more than moderate PMR, 26 had severe MR. Underlying etiology was flail leaflets in 31 patients and prolapse in 7; most lesions were in the PL (n = 31), 6 in the AL, 3 were bileaflet prolapse, and 4 were commissural lesions. Patients with PMR had larger regurgitant volume and effective regurgitant orifice area, but similar regurgitant fraction, compared with their SMR counterparts (Table 1). Mean age was lower in the normal group compared with both the PMR and SMR groups. LVEF was significantly different among the groups, being lowest in patients with SMR, intermediate in PMR, and highest in normal subjects (Table 1). Heart rate was slightly higher in the SMR group and comparable in normal subjects and patients with PMR. Systolic blood pressure was similar among the 3 groups. A total of 13 patients (7 in the SMR and 6 in the PMR groups) were in atrial fibrillation during the acquisition of the TEE images.

GEOMETRY OF THE MV ANNULUS AND LEAFLETS. The geometric parameters of the MV apparatus quantitated from 3D TEE (MV annulus and leaflets) are detailed in Table 2. MV annular area was significantly larger in both the SMR and PMR groups (12.7 ± 0.7 and 13.3 ± 0.7 cm^2, respectively) compared with that of normal subjects (9.9 ± 0.3 cm^2; $p < 0.05$). Similarly, total MV leaflet area was larger in the SMR (16.2 ± 0.9 cm^2) and PMR (15.6 ± 0.8 cm^2) groups versus normal subjects (11.6 ± 0.4 cm^2; both $p < 0.0001$), with no difference seen in total MV leaflet area between the SMR and PMR groups.

Regionally, AL surface area was largest in the SMR group, intermediate in PMR, and smallest in the normal group. In contrast, PL surface area was larger in patients with SMR and PMR compared with normal subjects (Table 2). The ratio of leaflet areas (PL over AL) was 0.9 ± 0.04 in SMR, similar to normal subjects

FIGURE 2 Strain Percentile Curves Reflecting the Regional Distribution of Strain on the Anterior and Posterior MV Leaflets in Normal Valves and in Patients With Primary and Secondary MR

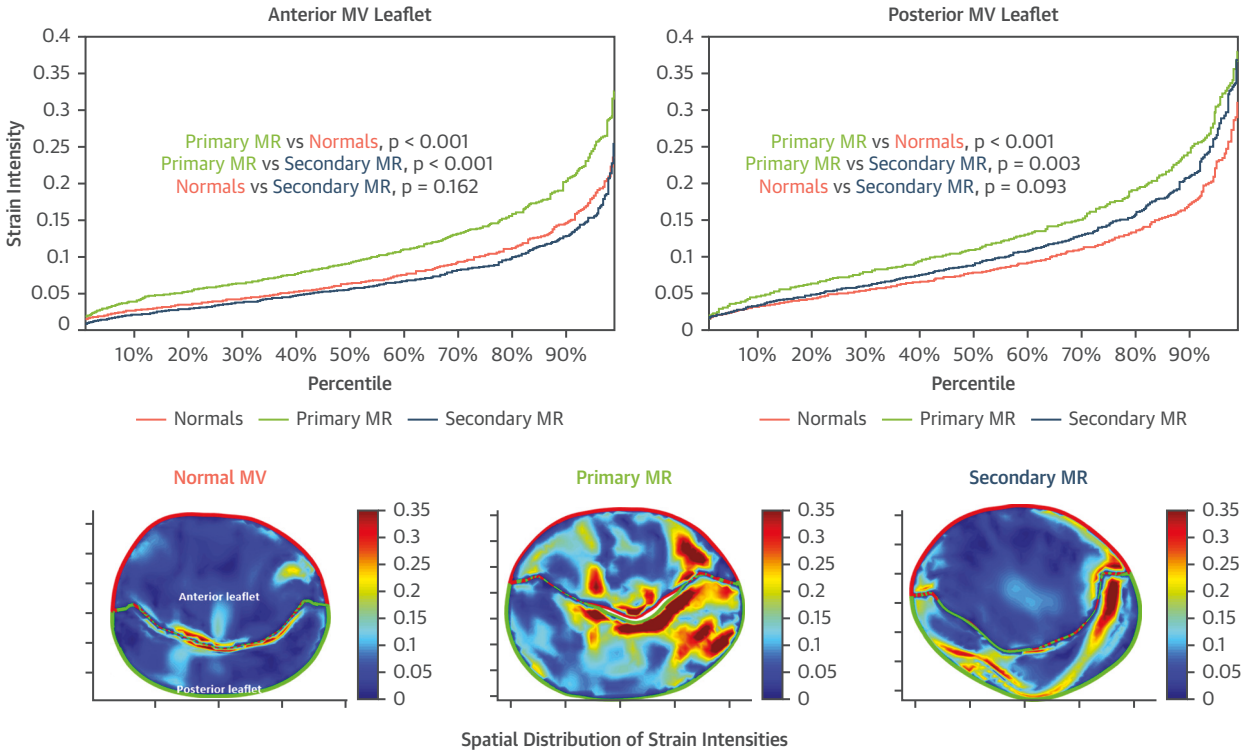

Strain percentile curves showing the percent of the approximately 800 analyzed points on the MV that have a strain value at or below the respective value on the curve for the group analyzed (e.g., 50th percentile is the median). MV strain was significantly higher in the primary MR group for both leaflets. MV strain values in secondary MR were overall similar to normal subjects. Example cases from each group are depicted in the lower diagrams as heat maps of isotropic strain along the surface of the MV. Abbreviations as in Figure 1.

(0.8 ± 0.04), indicating that remodeling occurred to the same degree in both leaflets in the SMR group. In contrast, PL/AL area ratio was largest in the PMR group (1.2 ± 0.07) compared with both normal subjects and SMR ($p < 0.001$), denoting a larger innate or growth of the posterior leaflet in PMR compared with the anterior leaflet in this group.

Leaflets had significantly higher thickness in both the SMR and PMR groups compared with that of normal subjects, both of the AL and PL (Table 2). Thickness of the AL was comparable in SMR and PMR; the PL was even thicker in PMR compared with SMR (Table 2).

MV LEAFLET STRAIN. Deformation analysis in the ALs and PLs was calculated and represented graphically as percentile strain distribution (Figure 2). Respective patient examples of MV strain heat maps from each group are also shown in Figure 2. Strain percentile in the AL trended lower in the SMR group compared with normal subjects but was highest in the PMR group. Strain in the PL was similar in the SMR group and normal subjects and was also highest in the PMR group. Therefore, despite a larger MV annulus and leaflet surface area, strain in the SMR group was not significantly different from that of the normal group.

Mean strain values for the total MV, the ALs and PLs leaflets for each group are shown in Figure 3. Mean strain values were significantly higher in the PL compared with the AL in all 3 groups: SMR (10.9 ± 0.4% vs. 6.8 ± 0.3%); PMR (13 ± 0.4% vs. 10.8 ± 0.4%); and normal MV (9.3 ± 0.4% vs. 7.6 ± 0.3%) ($p < 0.015$ for all). Despite significant MV apparatus remodeling in SMR, total MV strain was similar to normal valves (8.8 ± 0.3% vs. 8.5 ± 0.2%, but significantly lower than that in PMR (12 ± 0.4%; $p < 0.0001$).

In the group with MV prolapse ($n = 38$), prolapse and/or flail occurred in the PL in most patients ($n = 31$; 82%), which permitted the analysis of

FIGURE 3 MV Strain in Normals Valves and in Patients With Primary and Secondary MR

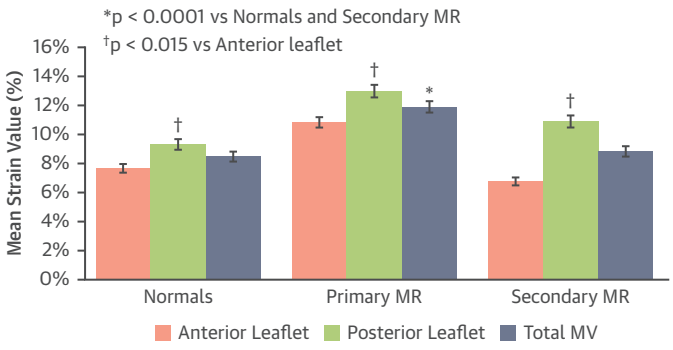

Mean total and leaflet specific MV strain values in normal subjects and patients with primary (PMR) and secondary MR (SMR). Mean strain of the posterior leaflet **(green bars)** is consistently higher than the anterior leaflet **(red bars)** across all groups. Mean total MV strain **(gray bars)** is highest in the PMR group, and similar between normal subjects and those with SMR. Error bars: ±1 SE. Abbreviations as in Figure 1.

regional strain differences in the involved scallops versus noninvolved scallops. Strain was significantly higher in the affected region compared with the nonaffected scallops ($p < 0.001$).

STRAIN IN ISCHEMIC VERSUS NONISCHEMIC SMR. In the SMR group ($n = 36$), there were 11 (31%) patients who had an ischemic etiology for their MR (i.e., ischemic leaflet tethering). Mean AL strain, mean PL strain, and mean total strain were all comparable between patients with ischemic MR and patients with nonischemic MR (6.7 ± 0.3% vs. 7.0 ± 0.5%; 10.7 ± 0.5% vs. 11.4 ± 0.7%; and 8.7 ± 0.3% vs. 9.2 ± 0.5%, respectively). The slightly lower strain in ischemic MR did not reach statistical significance.

CLINICAL AND IMAGING PARAMETERS ASSOCIATED WITH STRAIN. We sought to elucidate the potential clinical, echocardiographic, and geometric valve and annular parameters that were associated with mean MV strain. Table 3 displays the univariable and multivariable analyses of the correlates of valve strain in the total population. Valve thickness, severity of MR, and the presence of prolapse or flail were the univariate predictors of valve strain. MR severity and MR etiology were highly associated ($p < 0.001$). Because of collinearity between these 2 variables, we chose to drop MV prolapse and/or flail and include MR severity because it is common for both MV diseases; valve thickness was the only parameter associated with MV strain on multivariable analysis. The relationship between mean MV strain and leaflets thickness is depicted in Figure 4 ($r = 0.33$; $p < 0.001$). The regression lines for all patients and for those with SMR and PMR are shown separately, highlighting the lower strain values seen in SMR compared with PMR throughout the range of valve thickness (Figure 4). Because of the relation of MR severity to strain, we analyzed MV strain in patients with less than severe MR. In patients with moderate SMR, AL strain was lower than that in normal subjects (6.2 ± 0.3% vs. 7.6 ± 0.3%; $p < 0.001$), whereas AL strain in moderate PMR remained higher than that in normal subjects (9.6 ± 0.6% vs. 7.6 ± 0.3%; $p < 0.01$). In the posterior leaflets, moderate SMR strain was similar to normal subjects (10.2 ± 0.5% vs. 9.3 ± 0.3%, respectively; $p = 0.17$).

REPRODUCIBILITY. The interoperator strain distribution correlation was strong for both the ALs ($r = 0.90$) and PLs ($r = 0.83$). The absolute strain difference was 2 ± 0.3% for the AL and 1.7 ± 0.4% for the PL. In contrast, intraoperator correlation was strong for the ALs ($r = 0.93$) and the PLs ($r = 0.92$). The absolute strain difference was 1.7 ± 0.2% for the AL and 1.9 ± 0.2% for the PL. Strain percentile distribution along the ALs and PLs were comparable for both interoperator and intraoperator (the Kolmogorov-Smirnov p value was nonsignificant for ALs and PLs for both interoperator and intraoperator distributions).

DISCUSSION

In this investigation, real-time 3D TEE allowed the quantitation of patient-specific MV leaflet deformation in a population with regurgitant valves of various etiologies and normal subjects. MV geometric and strain models were generated using a combination of available and proprietary software. Patients with SMR had significant geometric remodeling of the MV apparatus, in leaflet area, annular dimensions, and leaflet thickness, similar to PMR, with the distinction that PL area was larger and thicker in PMR. MV strain was higher in the PL compared to that of the AL in all patient groups. Despite major MV remodeling in SMR, valve strain was similar overall to or slightly lower than normal and much lower than PMR (Central Illustration).

MV MODELING FOR STRAIN CALCULATION. Most of the earlier studies that evaluated MV deformation and leaflets tissue elastic properties were based on animal models in which crystals were surgically implanted on the MV and their motion tracked using dedicated cameras (1-3,6,7,9,12). Information on strain distribution on the surface of MV leaflets in humans is quite limited, involving a small number of patients. The saddle shape of the MV annulus was shown to increase leaflets curvature and contribute to

TABLE 3 Univariable and Multivariable Correlates of MV Strain

	Univariable		Multivariable	
	Estimated Coefficient (95% CI)	p Value	Estimated Coefficient (95% CI)	p Value
Mean leaflet thickness, mm	0.0199 (0.0088 to 0.0311)	0.001	0.0164 (0.0018 to 0.031)	0.028
MR severity				
No MR	Ref.		Ref.	
Moderate MR	0.0044 (−0.0134 to 0.0223)	0.624	−0.01 (−0.0318 to 0.0117)	0.362
Severe MR	0.0335 (0.0163 to 0.0508)	<0.001	0.0172 (−0.0051 to 0.0395)	0.13
Age	0.0001 (−0.0004 to 0.0001)	0.680		
SBP (mm Hg)	−0.0002 (−0.0005 to 0.0001)	0.131		
Sex	0.0022 (−0.0132 to 0.0176)	0.779		
LVEF (%)	−0.00005 (−0.0007 to 0.0006)	0.877		
Annulus area (cm^2)	0.0009 (−0.0009 to 0.0027)	0.320		
Annulus height (cm)	0.0076 (−0.0222 to 0.0373)	0.614		
Annulus area change (%)	−0.0005 (−0.0018 to 0.0009)	0.497		
MR etiology				
Normal	Ref.			
Prolapse	0.0511 (0.0191 to 0.0831)	0.002		
Flail	0.033 (0.015 to 0.051)	<0.001		
Ischemic	0.0073 (−0.0178 to 0.0325)	0.563		
Nonischemic	0.002 (−0.0172 to 0.0212)	0.837		

CI = confidence interval; other abbreviations as Tables 1 and 2.

reducing peak leaflet stress in 3 patients (6) and in animal valve models (4,6,26). Human MV models based on 10 normal subjects were used to emulate mitral leaflets deformation during isovolumic contraction (27). A MV model based on 3D echo images for 2 normal subjects and 2 patients with MR (10,11) aimed to model valve leaflet strain, assuming that papillary muscles remain at constant distance from the mitral leaflets (28,29). Because the in vivo biomechanical properties of human MV leaflets are not yet well quantified, all the previously mentioned investigations used elasticity model parameters derived from animal data (4,26).

In the present study, we quantitated MV leaflets strain and its regional distribution in regurgitant MV and normal subjects. It built on our recent pilot observations (13,14), and, with >100 patients, presented the largest MV strain data in humans. The tracking of the MV leaflets was automated, with minimal operator input required, mostly in PMR cases with flail or significant prolapse with a large malcoaptation gap. Patient-specific leaflet deformations were reconstructed by computerized diffeomorphic registration of the 3D echocardiography images. Computed strain was then systematically generated by leaflet dynamics at approximately 800 points on the MV (30). This enabled the comparative study of patient-specific strain distributions among patient groups.

Quantifying leaflet strain as indicator of MV tissue fatigue has several advantages. First, this approach can be easily implemented for human subjects through computer analysis of standard 3D echocardiography. Second, we did not need to introduce any elasticity hypotheses of MV leaflet tissue for strain calculation. Realistic MV elasticity models are anisotropic and highly nonlinear so that in most publications, parametrization of elasticity models for human MVs relies on stress measurements made in vivo on animal models. Comparison of MV strain distributions across patients is robust to reconstruction errors, because it relies on percentile curves computed from approximately 800 strain values for each leaflet, so that the error on any strain percentile is 20 times smaller than the errors affecting individual strain values.

STRAIN IN ANTERIOR VERSUS POSTERIOR MV LEAFLETS. In all MVs, including those in normal subjects and those with PMR and SMR, MV strain was found to be higher in the PL compared with the AL. This could be explained by the lower stiffness on the posterior aspect of the mitral annulus, as previously demonstrated histologically (31). May-Newman et al. (32), using excised porcine valves, demonstrated that the PL was more extensible than its anterior counterpart, with significantly higher strain attained at the same stress values. These findings, which are in line with our previous pilot data (13,14), are of particular clinical interest, because it is well established that most mitral annular calcifications occur in the posterior mitral annulus (33). In SMR, the higher strain in the PL is still observed. The repetitive regional deformation of relatively higher magnitude could hypothetically be a contributing mechanism to the

FIGURE 4 Mean MV Strain Versus Mean Leaflet Thickness, Color-Coded for Each MV Group

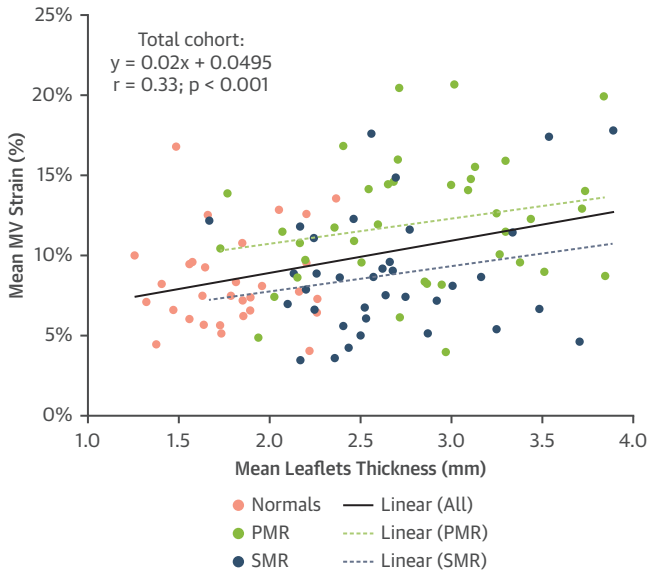

Mean MV strain correlates with leaflet thickness, which remains significant after adjustment for relevant variables. MV strain in SMR was lower than that of PMR throughout the range of valve thickness. Abbreviations as Figures 1 and 3.

observed posterior annular calcifications in the aging MV or in a milieu more susceptible to inflammation or calcification (e.g., renal disease).

MV STRUCTURE AND/OR REMODELING AND STRAIN. Both the SMR and PMR groups had significant remodeling of the MV apparatus. The MV annulus area and perimeter were larger and to a similar extent in both groups compared with that of normal subjects (Table 2). Leaflet surface area was also similarly larger in SMR and PMR compared with that of normal subjects, although with some differences regionally. In SMR, both the ALs and PLs were proportionally enlarged, preserving the PL/AL area ratio to <1 in normal subjects. In contrast, the larger leaflets in PMR predominantly involved the PL, altering the PL/AL area ratio to >1. Whether this is innate or part of the remodeling process in PMR could not be determined from the present study.

Despite a similarly remodeled MV apparatus in SMR and PMR, strain was higher in PMR in both the ALs and PLs, suggesting that the intrinsic properties of the MV (i.e., myxomatous degeneration in PMR) played a significant role in leaflet deformation (34). This was consistent with findings at pathology that showed higher intrinsic strain in myxomatous valves (35). In contrast, in patients with SMR, strain was overall comparable to normal subjects despite a larger annulus, leaflet surface area, and increased thickness. This finding was of interest, particularly in view of data at pathology that showed increased stiffness and thickness of such valves, likely because of higher collagen and glycosaminoglycans content (36–38). The finding of overall near-normal strain in SMR in the present study might be related to opposing factors on MV strain when evaluated in vivo; the increased annular area, leaflet area, and severity of MR might increase MV strain, modulating the intrinsic properties of the valve tissue in SMR (36–40). In patients with less severe MR, strain in the anterior leaflet in SMR was less than normal, unmasking some of the valve tissue properties in SMR. For similar valve thickness, strain was consistently lower in SMR compared with PMR (Figure 4).

Remodeling of the MV in response to changes in LV geometry and/or infarction is an active area of investigation (36–40). Recently, increased gene expression of matrix proteins and smaller leaflets were found in MVs of hearts with volume overload subjected to small apical infarctions, suggesting impaired adaptive valve growth and more SMR (39). The clinical impact of strain measurement in SMR, alone or in conjunction with altered geometric MV parameters and severity of MR, remains to be determined. Having the methodology to quantitate MV strain in vivo would facilitate such evaluation in the future.

STUDY LIMITATIONS. Leaflet thickness measurements might be limited by TEE's intrinsic spatial resolution and the methods we used in determining these values; we preferred to obtain an average thickness as opposed to a repeated linear thickness measurement that would increase variability. Strain is anisotropic in the MV, and the current area strain merged both radial and circumferential strain, so our conclusions might be limited by 2 factors—the high variability in strain within groups and the combining of radial and circumferential strains in the method used. However, in vitro data showed that in SMR and PMR, both directional strains were affected in the same direction, although with different magnitudes. Although we tried to incorporate as many parameters as possible into the multivariable analysis, we realize that other factors could be at play and were not fully captured by our analysis. Despite this being the largest MV strain study to date, the sample size in each group remained relatively small and further investigations are warranted to confirm strain determinants. Finally, the multibeat and high volume rate acquisitions on 3D TEE included data from at

CENTRAL ILLUSTRATION **Mitral Valve Strain in Secondary Mitral Regurgitation, Primary Regurgitation Due to Mitral Valve Prolapse and Normal Valves**

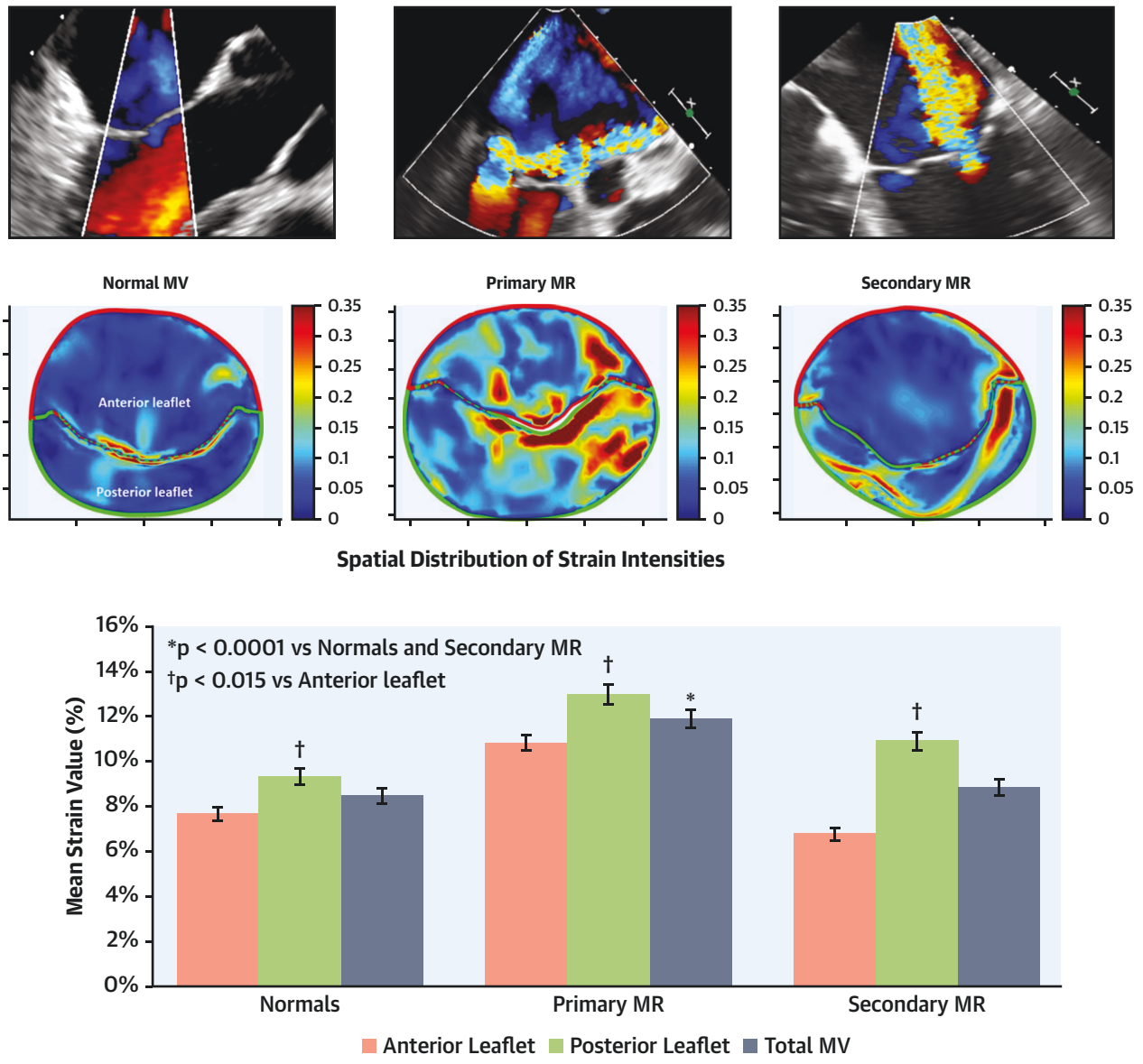

El-Tallawi, K.C. et al. J Am Coll Cardiol Img. 2021;14(4):782-93.

Mitral valve (MV) strain is highest in primary mitral regurgitation (MR) due to MV prolapse. Valve strain in secondary MR is overall similar to normal valves and may be lower on anterior leaflets in patients with less severe MR. Posterior MV leaflet strain is consistently higher than anterior leaflet strain, regardless of the presence or absence of MV disease.

most 4 consecutive beats. Although these beats could potentially have variable strain values, we assumed that those differences were negligible because the beats were consecutive, in the setting of a stable heart rate, blood pressure, patient motion, and respiratory effort.

CONCLUSIONS

This was the largest study in humans in which patient-specific strain was quantified noninvasively on MV leaflets. Patients with SMR had significant valve remodeling and increased valve thickness,

JACC: CARDIOVASCULAR IMAGING, VOL. 14, NO. 4, 2021
APRIL 2021:782–93

similar to PMR and yet had close to, or in some instances, lower strain than normal, but consistently lower than PMR, paralleling the biochemical changes observed at pathology. Strain was higher in the PL in all MV, supporting the predilection of the PL and annulus to disease states. With the availability of MV strain calculations, longitudinal studies are needed to assess the prognostic impact of MV strain in patients with MV disease and its possible implications in valve interventions.

FUNDING SUPPORT AND AUTHOR DISCLOSURES

This study was supported by the Elkins Family distinguished Chair in cardiac health, and the John and Maryanne McCormack Cardiology Fund. The authors have reported that they have no relationships relevant to the contents of this paper to disclose.

ADDRESS FOR CORRESPONDENCE: Dr. William A. Zoghbi, Department of Cardiology, Houston Methodist DeBakey Heart and Vascular Center, 6550 Fannin Street, SM 1801, Houston, Texas 77030, USA. E-mail: wzoghbi@houstonmethodist.org.

PERSPECTIVES

COMPETENCY IN MEDICAL KNOWLEDGE: Most previously published MV leaflet deformation studies were performed in animal models. Our study explored the geometric and deformation characteristics in patients with SMR compared with those with PMR and normal subjects. Patients with SMR had larger and thicker valves, larger annuli but similar strain, and in some instances, lower than normal valves. Strain was highest in PMR. Valve thickness, severity of MR, and primary etiology of MR were correlates of strain, with leaflet thickness being the multivariable parameter significantly associated with MV strain.

TRANSLATIONAL OUTLOOK: Our noninvasive quantitative strain approach adds to the armamentarium of MV assessment tools by opening a new window to evaluate and potentially detect subclinical MV disease. Further studies are needed to establish the prognostic impact of strain in the natural history of SMR and PMR or after valve interventions.

REFERENCES

1. Jimenez JH, Liou SW, Padala M, et al. A saddle-shaped annulus reduces systolic strain on the central region of the mitral valve anterior leaflet. J Thorac Cardiovasc Surg 2007;134:1562–8.

2. Amini R, Eckert CE, Koomalsingh K, et al. On the in vivo deformation of the mitral valve anterior leaflet: effects of annular geometry and referential configuration. Ann Biomed Eng 2012;40:1455–67.

3. Padala M, Hutchison RA, Croft LR, et al. Saddle shape of the mitral annulus reduces systolic strains on the P2 segment of the posterior mitral leaflet. Ann Thorac Surg 2009;88:1499–504.

4. Ryan LP, Jackson BM, Hamamoto H, et al. The influence of annuloplasty ring geometry on mitral leaflet curvature. Ann Thorac Surg 2008;86:749–60; discussion 749–60.

5. Kunzelman KS, Reimink MS, Cochran RP. Annular dilatation increases stress in the mitral valve and delays coaptation: a finite element computer model. Cardiovasc Surg 1997;5:427–34.

6. Salgo IS, Gorman JH 3rd., Gorman RC, et al. Effect of annular shape on leaflet curvature in reducing mitral leaflet stress. Circulation 2002;106:711–7.

7. Rausch MK, Bothe W, Kvitting JP, Goktepe S, Miller DC, Kuhl E. In vivo dynamic strains of the ovine anterior mitral valve leaflet. J Biomech 2011;44:1149–57.

8. Stevanella M, Krishnamurthy G, Votta E, Swanson JC, Redaelli A, Ingels NB Jr. Mitral leaflet modeling: importance of in vivo shape and material properties. J Biomech 2011;44:2229–35.

9. He Z, Ritchie J, Grashow JS, Sacks MS, Yoganathan AP. In vitro dynamic strain behavior of the mitral valve posterior leaflet. J Biomech Eng 2005;127:504–11.

10. Rim Y, McPherson DD, Chandran KB, Kim H. The effect of patient-specific annular motion on dynamic simulation of mitral valve function. J Biomech 2013;46:1104–12.

11. Rim Y, Laing ST, Kee P, McPherson DD, Kim H. Evaluation of mitral valve dynamics. J Am Coll Cardiol Img 2013;6:263–8.

12. Sacks MS, He Z, Baijens L, et al. Surface strains in the anterior leaflet of the functioning mitral valve. Ann Biomed Eng 2002;30:1281–90.

13. Ben Zekry S, Freeman J, Jajoo A, et al. Patient-specific quantitation of mitral valve strain by computer analysis of three-dimensional echocardiography: a pilot study. Circ Cardiovasc Imaging 2016;9:e003254.

14. Ben Zekry S, Freeman J, Jajoo A, et al. Effect of mitral valve repair on mitral valve leaflets strain: a pilot study. J Am Coll Cardiol Img 2018;11:776–7.

15. Zoghbi WA, Adams D, Bonow RO, et al. Recommendations for noninvasive evaluation of native valvular regurgitation: a report from the American Society of Echocardiography Developed in Collaboration with the Society for Cardiovascular Magnetic Resonance. J Am Soc Echocardiogr 2017;30:303–71.

16. Cao Y, Miller MI, Winslow RL, Younes L. Large deformation diffeomorphic metric mapping of vector fields. IEEE Trans Med Imaging 2005;24:1216–30.

17. Helm P, Beg MF, Miller MI, Winslow RL. Measuring and mapping cardiac fiber and laminar architecture using diffusion tensor MR imaging. Ann N Y Acad Sci 2005;1047:296–307.

18. Mansi T, Peyrat J, Sermesant M, et al. Physically-constrained diffeomorphic demons for the estimation of 3D myocardium strain from cine-MRI. In: Ayache N, Delingette H, Sermesant M, editors. Functional Imaging and Modeling of the Heart. Heidelberg, Germany: Springer, 2009;5528:201–10.

19. Lombaert H, Peyrat J, Croisille P, et al. Human atlas of the cardiac fiber architecture: study on a healthy population. IEEE Trans Med Imaging 2012;31:1436–47.

20. Heyde B, Alessandrini M, Hermans J, Barbosa D, Claus P, D'hooge J. Anatomical image registration using volume conservation to assess cardiac deformation from 3D ultrasound recordings. IEEE Trans Med Imaging 2015;35:501–11.

21. Prakosa A, Mcleod K, Sermesant M, Pennec X. Evaluation of ilogdemons algorithm for cardiac motion tracking in synthetic ultrasound sequence. In: Statistical Atlases and Computational Models of the Heart. Imaging and Modelling Challenges. New York: Springer, 2012; p 178–87.

22. Azencott R, Glowinski R, Ramos AM. A controllability approach to shape identification. Appl Math Lett 2008;21:861–5.

23. Azencott R, Glowinski R, He J, et al. Diffeomorphic matching and dynamic deformable surfaces in 3D medical imaging. Comput Methods Appl Math 2010;10:235–74.

24. Zekry SB, Lawrie G, Little S, et al. Comparative evaluation of mitral valve strain by deformation tracking in 3D-echocardiography. Cardiovasc Eng Technol 2012;3:402–12.

25. Weiss MS. Modification of the Kolmogorov-Smirnov statistic for use with correlated data. J Am Stat Assoc 1978;73:872–5.

26. Ryan LP, Jackson BM, Eperjesi TJ, et al. A methodology for assessing human mitral leaflet curvature using real-time 3-dimensional echocardiography. J Thorac Cardiovasc Surg 2008;136:726–34.

27. Xu C, Brinster CJ, Jassar AS, et al. A novel approach to in vivo mitral valve stress analysis. Am J Physiol Heart Circ Physiol 2010;299:H1790–4.

28. Joudinaud TM, Kegel CL, Flecher EM, et al. The papillary muscles as shock absorbers of the mitral valve complex. An experimental study. Eur J Cardiothora Surg 2007;32:96–101.

29. Sanfilippo AJ, Harrigan P, Popovic AD, Weyman AE, Levine RA. Papillary muscle traction in mitral valve prolapse: quantitation by two-dimensional echocardiography. J Am Coll Cardiol 1992;19:564–71.

30. Slaughter WS, editor. The Linearized Theory of Elasticity. Boston, MA: Springer, 2002.

31. Gunning GM, Murphy BP. Determination of the tensile mechanical properties of the segmented mitral valve annulus. J Biomech 2014;47:334–40.

32. May-Newman K, Yin FC. Biaxial mechanical behavior of excised porcine mitral valve leaflets. Am J Physiol 1995;269:H1319–27.

33. Bloom N, Cashon G. Annulus fibrosus calcification of the mitral valve. Am Heart J 1945;30:619–22.

34. El Tallawi KC, Zhang P, Azencott R, et al. Quantitation of mitral valve strain in normals and in patients with mitral valve prolapse. J Am Coll Cardiol 2019;73 Supp 1:1953.

35. Barber JE, Kasper FK, Ratliff NB, Cosgrove DM, Griffin BP, Vesely I. Mechanical properties of myxomatous mitral valves. J Thorac Cardiovasc Surg 2001;122:955–62.

36. Grande-Allen KJ, Borowski AG, Troughton RW, et al. Apparently normal mitral valves in patients with heart failure demonstrate biochemical and structural derangements: an extracellular matrix and echocardiographic study. J Am Coll Cardiol 2005;45:54–61.

37. Grande-Allen KJ, Barber JE, Klatka KM, et al. Mitral valve stiffening in end-stage heart failure: evidence of an organic contribution to functional mitral regurgitation. J Thorac Cardiovasc Surg 2005;130:783–90.

38. Timek TA, Lai DT, Dagum P, et al. Mitral leaflet remodeling in dilated cardiomyopathy. Circulation 2006;114(I):518–23.

39. Marsit O, Clavel M, Côté-Laroche C, et al. Attenuated mitral leaflet enlargement contributes to functional mitral regurgitation after myocardial infarction. J Am Coll Cardiol 2020;75:395–405.

40. Howsmon DP, Rego BV, Castillero E, et al. Mitral valve leaflet response to ischaemic mitral regurgitation: from gene expression to tissue remodelling. J Royal Soc Interface 2020;17:20200098.

KEY WORDS **echocardiography, mitral valve, strain, valve regurgitation**

APPENDIX **For an expanded Methods section, please see the online version of this paper.**